Variable-Stiffness Tensegrity Spine

Davide Zappetti*, Roc Arandes*, Enrico Ajanic, Dario Floreano

The authors are with the Laboratory of Intelligent Systems, School of Engineering, Ecole Polytechnique Fédérale de Lausanne, 1015 Lausanne, Switzerland.
* These authors contributed equally to this work

E-mail: davide.zappetti@epfl.ch; roc.arandes@epfl.ch

***Abstract*—Vertebrates including amphibians, reptiles, birds and mammals, with their ability to change stiffness of the spine to increase load-bearing capability or flexibility, have inspired roboticists to develop artificial variable-stiffness spines. However, unlike their natural counterparts, current robotic spine systems do not display robustness or cannot adjust their stiffness according to their task. In this paper, we describe a novel variable-stiffness tensegrity spine, which uses an active mechanism to add or remove a ball-joint constrain among the vertebrae, allowing transition among different stiffness modes: soft mode, global stiff mode and directional stiff mode. We validate the variable-stiffness properties of the tensegrity spine in experimental bending tests and compare results to a model. Finally, we demonstrate the tensegrity spine system as a continuous variable-stiffness manipulator and highlight its advantages over current systems.**

I. Introduction

Robot bodies made from rigid parts can withstand high loads, but lack deformability [1]. Contrarily, soft robots can adapt to the environment by complying with obstacles and objects, yet, they lack strength due to their soft nature [2]. Ideally, robots should possess the ability to change between stiffness states depending on their surrounding environment and task. To address this tradeoff, roboticists have taken inspiration from the high mechanical adaptability of vertebrates. In all vertebrates, including amphibians, reptiles, birds and mammals, the spine plays a central role in mechanical adaptability. On one hand, the spine can increase its stiffness to support the body's weight and provide load-bearing capabilities. On the other hand, it can adaptively decrease stiffness to enable adaptive motion and provide flexibility when necessary [3].

New biological studies have highlighted the mechanical complexity of biological spines that are composed of not only rigid components under compression (vertebrae) with pivots functioning as joints, but also of intervertebral muscles that are under tension [3-5]. These muscles help to distribute loads and increase the robustness of the whole system (Figure 1(a)) [5]. The biological spine has a pre-defined bending stiffness given by the intervertebral muscles at rest, that can globally increase when all muscles are simultaneously actuated, pulling the vertebrae against each other [4].

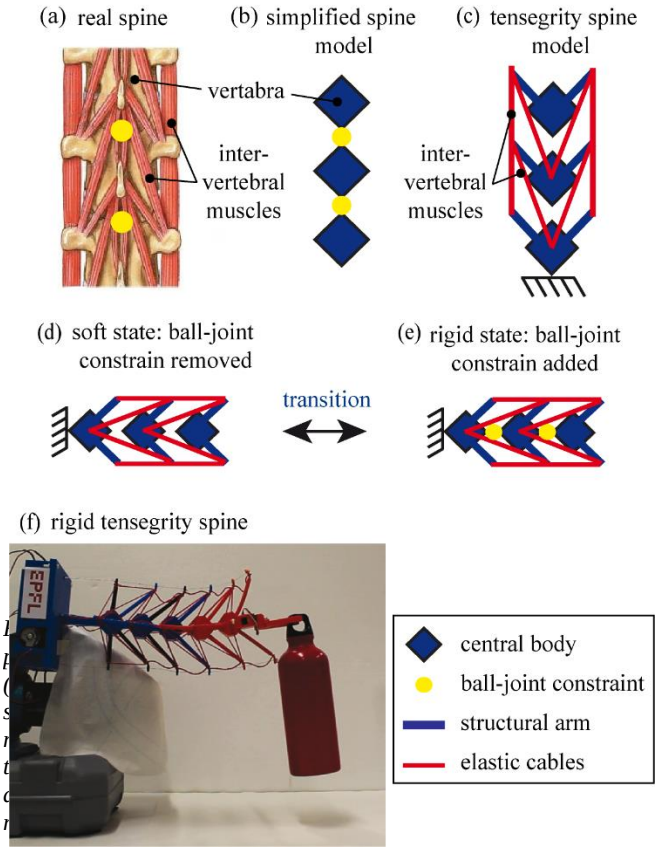

Furthermore, directional bending stiffness, i.e. selective compliance in one direction, is attained by actuating only selected muscles [4-5].

Several artificial spines with variable-stiffness capabilities have been developed and implemented in robotic systems. However, their design is often based on a largely simplified spine model where the spine is represented as a pillar of vertebrae interconnected by ball-joint constraints, but without intervertebral muscles (Figure 1(b)) [6-10]. Other spine systems are based on a tensegrity-truss system where the rigid vertebrae are stabilized by intervertebral muscles (i.e. pre-stretched elastic cables) [11-15]. However, the lack of ball-joint constrains in these systems does not allow the adaptation of the spine stiffness by pulling the vertebrae against each other (Figure 1(c)).

In this paper, we propose and investigate a novel tensegrity spine with variable-stiffness capabilities. The variation in stiffness is achieved by a mechanism that actively adds (Figure 1(f)) or removes (Figure 1(e)) a ball-joint constrain among the vertebrae and therefore allows to modulate the system's stiffness. We implement the variable-stiffness strategy in an actuated variable-stiffness tensegrity spine, which can transition between different bending stiffness modes: *soft*, *global stiff* and *directional stiff* as in its biological counterpart. We demonstrate the spine capabilities in the form of a continuous manipulator (Figure 1(f)), which can adapt its mechanical stiffness.

II. VARIABLE-STIFFNESS SPINE DESIGN

In this section, the variable-stiffness design strategy is introduced, followed by a detailed presentation of the hardware implementation in a variable-stiffness tensegrity spine segment. Finally, the different stiffness modes exhibited by the tensegrity spine are described.

A. Class-changing variable-stiffness strategy for tensegrity systems

The word tensegrity comes from the conjunction of the two words: *tension* and *integrity*. A tensegrity system can be defined as a set of rigid bodies that are connected and stabilized by tensile elements to form a mechanical structure [16]. Various classes of stable tensegrity structures that fit this definition exist. In *class 1* tensegrity system, the rigid bodies are not in contact and do not have ball-joint constraints (Figure 1(d)); in *class 2* tensegrity systems at least two rigid bodies are constrained by a ball-joint constraint [16] (Figure 1€). A *class 1* tensegrity structure is stable in a three-dimensional space thanks to the cable network. By adding ball-joint constraints, it is possible to augment its resistance to deformations and therefore increase its stiffness [16]. Our novel variable-stiffness strategy relies on the principle of transitioning from a *class 1* tensegrity system where the rigid bodies, i.e. the vertebrae, are not in contact with each other, to a stiffer *class 2* tensegrity spine with ball joint constraints among the rigid bodies (Figure 1(e)). We applied this strategy to a well-known *class 1* model of a spine, named *Tetrahedral Tensegrity Spine* [11-13], and included a mechanism to add constraints between the vertebrae when a stiffer configuration is required. The mechanism is described in detail in the section C.

B. Hardware implementation

The simplest stable *Tetrahedral Tensegrity Spine* is composed of an internal vertebra suspended in a network of tensioned cables connected to two external vertebrae at the top and at the bottom (Figure 2(b)). The vertebrae of our variable-stiffness tensegrity spine, similarly to the ones of the *Tetrahedral Tensegrity Spine* with a fixed stiffness, are composed of two main components: the *central body and* the *structural arms*. (Figure 2(a)). The *central body* facilitates the positioning and the assembly of four *structural arms* for each vertebra. The *structural arm tips* serve as vertices where tensile elements are attached to stabilize the structure.

In order to provide the mechanism with variable-stiffness, we add a pin with a spherical tip at the bottom face of the vertebra's central body; the spherical pin tip can fit a socket shaped into the top face of the central body. The resulting stiffness adaptation will be described in detail in section C. All the components of the vertebrae are made of polylactic acid (PLA) with a Stratasys DimensionElite 3D-printer and are manually connected with hot glue. The vertebrae arms are 50 mm long and with a cross section diameter of 2 mm. The distances between end tip of the arms and the geometrical center of a central body is 60 mm.

The tensioned cables to stabilize the three vertebrae of the spine present the same configuration design as described in [11-13] for the *Tetrahedral Tensegrity*. However, we designed cable tensile elements as a flat network that can be folded into the three dimensional (3D) spine structure, as we [17] and other authors [18] recently proposed. Our methodology [17] allows to easily manufacture the cables with 3D-printed thermoplastic polyurethane (TPU), which has the required elastic properties. The network is first designed with the help of computational aided design (CAD) for the three-vertebrae spine. Then, the unfolded network can be retrieved by eliminating the vertebrae and rotating the cables until a flat configuration is obtained (Figure 2(b)). The *tensile-element* network has a cross-section of 1 mm^2 and each cable is designed to exhibit a 10% pre-stretch when assembled. Although the presented assembled spine is a 3-vertebrae segment (Figure 2(c)), it can be extended by adding n-internal vertebrae and extending the cable network.

To change the stiffness and to actively bend the spine in the vertical plane, we implemented a tendon-driven actuation system (Figure 2(d)). This system is composed of four tendons made of Dyneema wires (ultra-high molecular weight polyethylene with a rigid Young Modulus of approximately 110GPa), each actuated by a DC electrical motor (DC12V25RPM from Pololu) and controlled by an Arduino Uno microcontroller (Figure 2(d)). Each of the four tendons is running in parallel to one of the four vertical elastic cables symmetrically displayed at four edges along the height of the spine (Figure 2(d)). The cables are fixed to the tip of top vertebra's arms (Figure 2(d)) while they run freely throughout holes in the tips of the bottom vertebrae's arms. The DC motors have been placed at the base of the tensegrity spine to which the first vertebrae is rigidly attached.

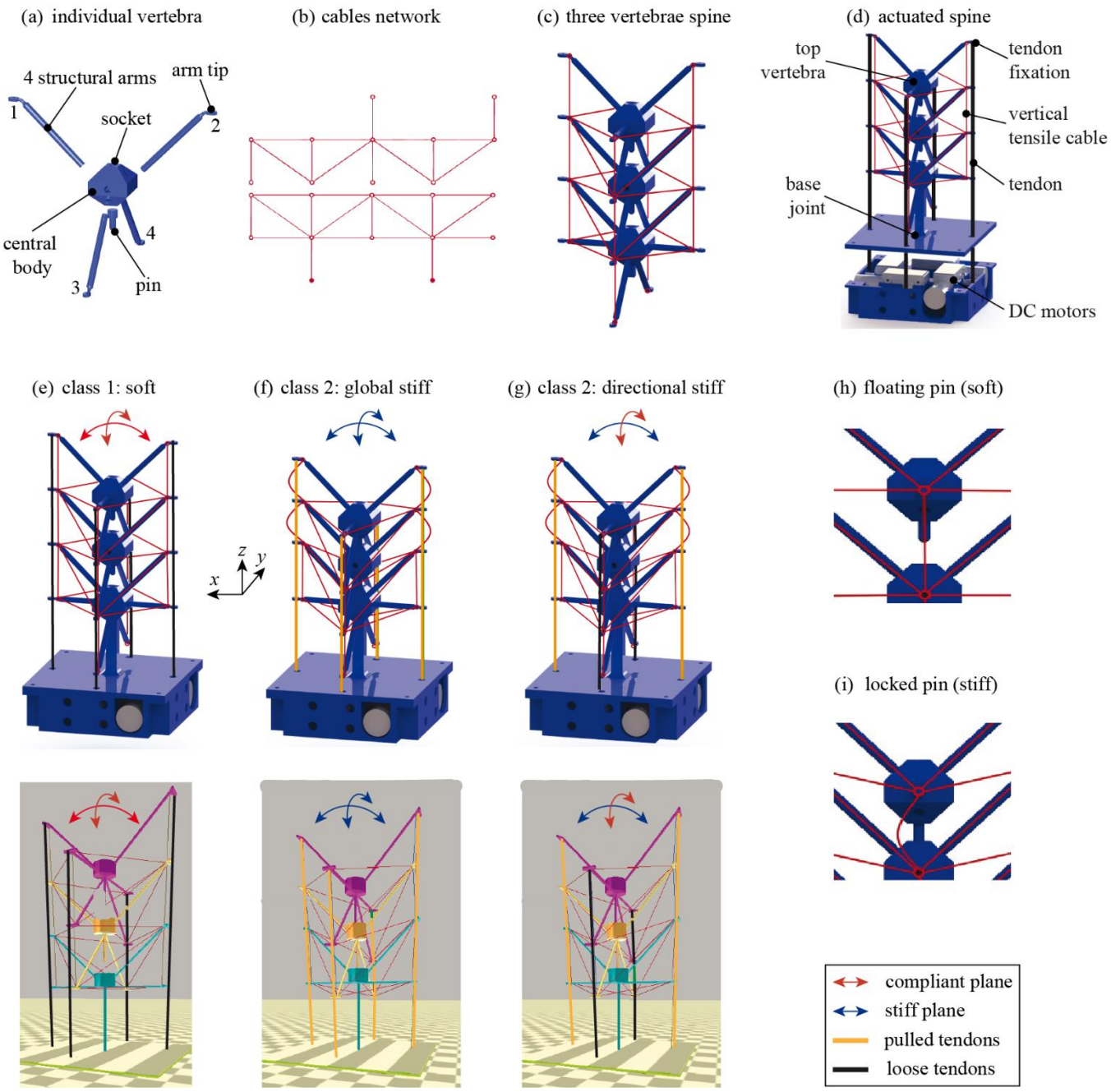

Figure 2. The upper part of the figure presents the variable-stiffness spine hardware implementation in detail. (a) Exploded view of a vertebra design. The numbers highlight the four structural arms. (b) The flat elastic network to assemble a three vertebrae spine segment. (b) The assembled 3 vertebrae spine segment. (d) Exploded view of the spine base containing the motor actuators and in black the four tendons connecting the top vertebra arm's tips to the motor actuators in the base. (e-f) Representation of the three stiffness modes both in hardware prototype and simulation model. The arrows represent the two orthogonal planes where the four tendons stand. The red arrows represent a compliant plane of bending, while blue arrows represent a stiff plane of bending. Green lines represent pulled tendons while black lines loose tendons. (e) The four tendon are loose and the spine is compliant in the two planes. (f) The four tendon are pulled and the spine is stiff in the two planes. (g) Two tendons are loose and two are pulled. The plane where the two loose cables stand is compliant the other is stiff.(h-i) Detailed 2D view of the pin floating in the soft mode and inserted in the socket in the stiff modes.

C. Stiffness transition mechanism and spine stiffness modes

In our modified spine design, the variable-stiffness is achieved by removing or adding ball-joint constrains between the vertebrae. According to which tendons are pulled, the tensegrity spine can transition between three different stiffness modes: *soft mode, global stiff mode, and directional stiff mode* (Figure 2(e-g)).

- Soft mode: When all the tendons are loose and the pins are not inserted (Figure 2(h)), the vertebrae are stabilized in space only by the elastic cables and with small loads can experience relative translations and rotations (Figure 2(e)). The tensegrity system is *class 1*.
- Global stiff mode: When the four tendons are pulled simultaneously, the *spherical pins* are inserted in the *sockets* of the underneath vertebrae adding a ball-joint constrain among the vertebrae and locking relative translations (Figure 2(i)), while the rigid pulled tendons constrain relative rotations in all longitudinal planes (Figure 2(f)). The tensegrity spine is a *class 2* tensegrity system.
- Directional stiff mode: When two opposite tendons are simultaneously pulled, the *spherical pins* are inserted in the *sockets* of the underneath vertebrae constraining relative translations (Figure 2(i)), while the two rigid tendons constrain relative rotations only in the plane where they stand. The bending in the orthogonal plane is constrained by the elastic cables that allow deformations (Figure 2(g)). The tensegrity spine is a *class* 2 tensegrity system.

In each of the three modes, it is possible to actively control the spine bending with the same actuation system. The bending can be controlled in four directions by pulling individually one of the four tendons (Figure 4(a)).

III. MODEL

To investigate the three stiffness modes, we developed a model of the spine using the NASA Tensegrity Robotics Toolkit (NTRT) [19]. The NTRT is an open source software package for modeling, simulation, and control of tensegrity robots based on the Bullet Physics engine [20]. Both kinematics and dynamics of the simulator have been validated and extensively used in prior works [21-23],

Similar to the hardware prototype, the model consists of a three-vertebrae tensegrity spine segment with four tendons running through holes at the tips of the vertebrae arms and attached to the tip of top vertebrae arms (Figure 2(e)). The vertebrae are modelled with arms as cylindrical rods of length 50 mm, and the distance of 60 mm between end arms tips and geometrical center of the central body is respected. At the arms tips of central and bottom vertebrae a hole through which the tendons run is approximated with a three-rod hollow triangle because of simulator limitations. The density of all vertebrae components is *1.25 g/cm3*, an approximation of the 3D printed PLA density. Likewise, in the hardware prototype, the bottom vertebra is rigidly constrained to a square base. The elastic cable network is modelled as a set of cables between the vertebrae arms tips with a Young's Modulus of 12.5 MPa corresponding to the value of the 3D printed TPU. Their pre-stretch is set to match the 10% of the real prototype. The tendons are modelled with a Young modulus of 110 GPa like their hardware counterparts.

To simulate the *soft mode*, the four tendons are not pulled (Figure 2(e)), while to simulate the *global and the directional stiff modes*, the tendons are pulled until the pins touch the upper faces of the central bodies of the underneath vertebrae (Figure 2(f) and 2(g)). Given the difficulty to model the round tip of the pin and concave shape of the socket, a translational constrain (i.e. a constrain that locks in plane movements of the pin's tip, while allowing rotations) is added between the tip of the pin and the center of the upper face of the bottom vertebra. Such a constrain is used to model the real constrain of the pin insertion in the socket.

IV. RESULTS

To validate the variable-stiffness strategy and the three stiffness modes, we performed load-displacement bending characterization in both reality and simulation (Section A), followed by the reachable workspace characterization of the actively controlled spine bending in each of the three modes (Section B).

A. Load-displacement bending characterization

For the hardware bending experiments, we fixed the tensegrity spine's base and applied loads F_x and F_y along the orthogonal planes to the last vertebra (i.e. planes x-z and y-z) by an Instron testing machine (5960 Series), which caused displacements in the x and y directions (Figure 3(a)), this allows to calculate bending stiffness in *x* and *y* directions. The same conditions were applied to the model. For this study, in all experiments the maximum displacement was $x = y = 5$ mm to stay abreast of the small angle approximation and linear load-displacement range.

Three different stiffness modes were tested. In the *soft mode* all actuation tendons were relaxed (Figure 3(a), green). In the *stiff mode* all tendons were pulled by a symmetric force until the pins entered their sockets (Figure 3(a), blue). In the *directional stiffness mode*, only two opposite tendons in the x-z plane were pulled until the pins entered the sockets (Figure 3a, red). For the latter two modes the stiffness of the system could be further increased by applying a greater tendon force *Ft*. However, this further stiffening of the system has already been widely discussed in [6], [7], [9] and thus it is not investigated in this paper.

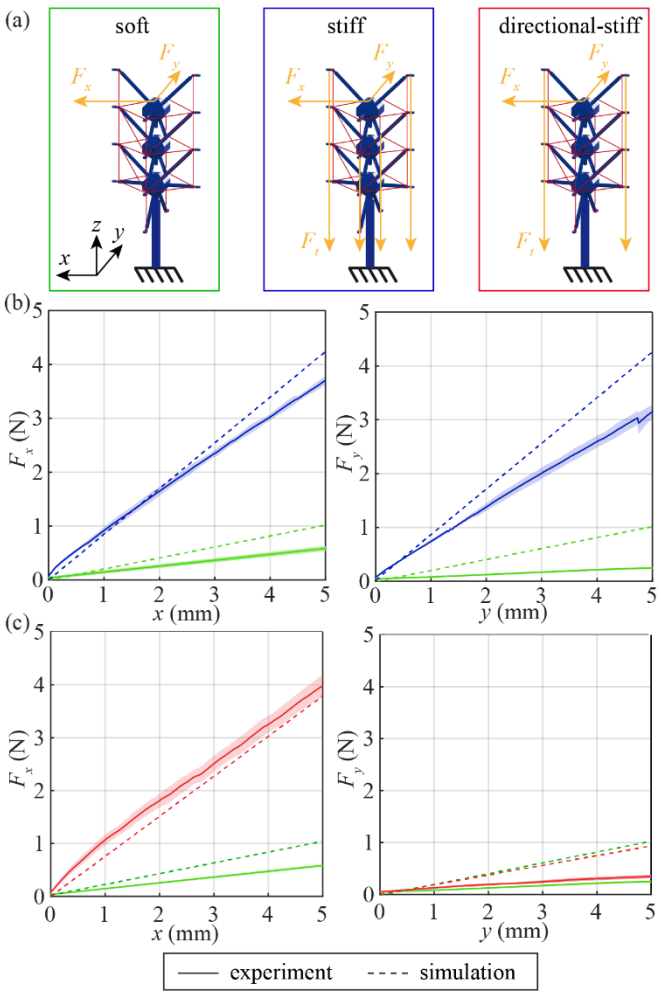

Figure 3. Results of the bending load characterization with the experimental setup in (a). The results of the experiment (solid lines) and the simulation (dashed lines) are shown in (b) for the soft (green) and stiff (blue) mode in the x-z-plane (force F_x, displacement x) and in the y-z-plane (force F_y, displacement y). (c) shows the results of the experiment and the simulation for the soft and directional stiff (red) modes in the x-z-plane (force F_x, displacement x) and in the y-z-plane (force F_y, displacement y). The shaded areas represent the standard deviation of the experimental measurements.

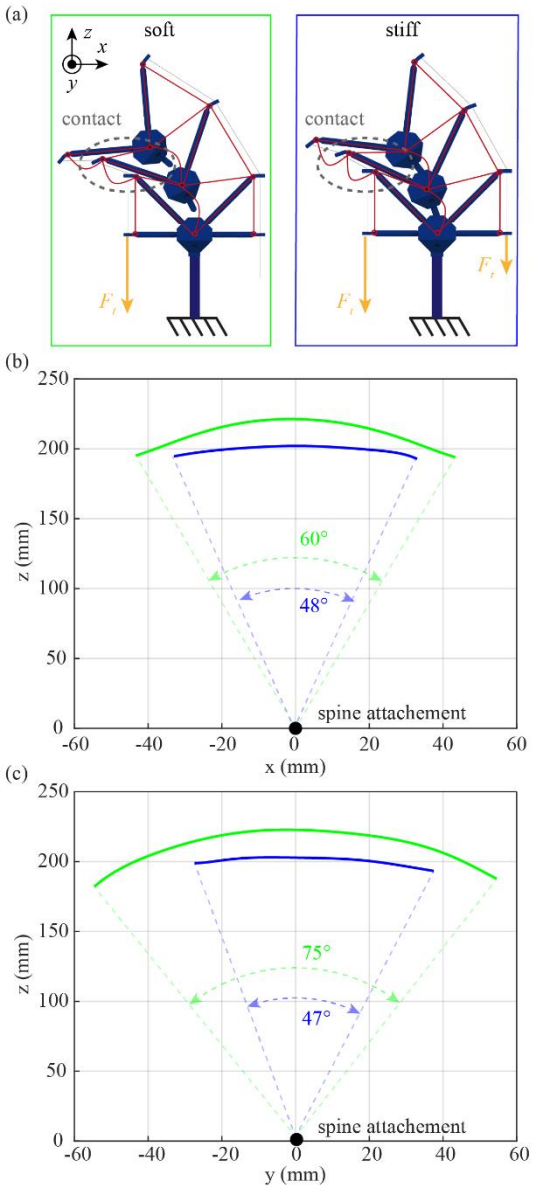

Figure 4. In the workspace experiment, the soft and stiff mode were considered as shown in the schematic in (a) and the bending was induced by applying a force F_t and pulling the tendon on one side, or asymmetrically on both sides, respectively. The measured trajectory of the central point of the upper face of the top vertebra in the x-z-plane for soft (green) and stiff (blue) are represented by the solid lines in (b), while the trajectories of the last vertebra in the y-z-plane for soft and stiff are shown by the solid lines in (c).

The experimental results confirm that in the stiff mode (Figure 3(b), blue) the bending stiffness can be increased by a factor of approximately six times the bending stiffness in the soft mode (Figure 3(b), green). The bending stiffness in the y-direction shows a decreased stiffness as compared to the x-direction. This could be explained by mechanical imperfections of the prototype that result in asymmetric stiffness. The slight deviations of the measured forces between the hardware and the model are probably due to slightly loose tendons fixations caused by manual knotting and to the 3D printing (Figure 2(b)) of the elastic cables that result in non-uniform cross-sectional areas. By pulling only the two tendons in the x-z-plane it is possible to achieve directional bending stiffness (Figure 3(a), red). When movement in this plane is constrained (similar to figure 3(b) right), the bending stiffness in x-direction is increased (Figure 3(c) left), while, the bending in the y-direction exhibits a stiffness comparable to the soft state.

B. Workspace experiments

By pulling individually one of the four tendons of the actuation mechanism, it is possible to actively control the spine bending. To assess how the stiffness modes influence the reachable workspace (i.e. maximum bending angles of the spine segment in the four actuated directions), we investigated the workspace of the variable-stiffness spine segment in soft mode and global stiff mode, assuming that the workspace of

the directional stiff mode is a combination of the two (i.e. same maximum bending angle of the stiff mode reachable in the stiff plane and maximum bending angle of the soft mode reachable in soft direction). The bending experiments are conducted by pulling only one tendon at a time in each mode until the external arms get in contact preventing any further bending (Figure 4(a)). A human operator can control the motors rotations that pull the tendons throughout an Arduino interface. The interface allows to apply small incremental rotations (i.e. 90°) to the motors until desired positions are reached. In order to track the movement of the system with an Optitrack motion capture system (solid lines in figure 4(b) and 4(c)), four reflector markers are fixed at the base of the tensegrity spine system as a reference, while one reflector marker is attached on the upper face of the top vertebra's central body. The trajectories are measured in the x-z-plane and the y-z-plane, as shown in figure 4 (solid lines).

The results show that a trade-off exists between stiffness and workspace. The measured workspace angle in the stiff mode is 20% smaller for the x-z-plane and 37% smaller in the y-z plane compared to the soft mode. The main reason for this decreased workspace angle between soft and stiff mode lies in the compression of the spine. When the spherical pins touch the central bodies, the distances between the vertebrae are reduced (see figure 2(e-g)) and consequently the radius of their relative rotation is shorter. The bending angles in positive and negative direction of both orthogonal planes are not perfectly symmetric. These differences can be explained by small asymmetries of the assembled spine or errors of the human operator that manually actuated the motors.

V. A CONTINUOUS TENSEGRITY MANIPULATOR

In order to demonstrate the potential of the variable-stiffness tensegrity spine in its different stiffness modes, we developed a continuous tensegrity manipulator based on the variable-stiffness tensegrity spine described above.

The manipulator is composed of a 5-vertebra, variable-stiffness tensegrity spine with a modified top vertebra equipped with a gripper (Figure 5(a) and 5(b)). The total height of the manipulator is 400 mm from top of the base to the tip of the gripper. The gripper is based on an open source design [24]. It is composed of a servomotor driven claw that can close and open to grasp objects (Figure 5(b)). The four motors of the tendon-driven actuation system and the servo are driven by an Arduino UNO and four L928N motor drivers (Figure 5(c)). A human operator, thanks to an Arduino Uno user interface, can control the manipulator. The human operator can bend the manipulator in four directions by pulling one individual tendon, or control the transition from the *soft mode* to the *global stiff mode* by pulling all four tendons at the same time, or change to the *directional stiff mode* by pulling only two opposite tendons at the same time.

The three different stiffness modes of the manipulator are demonstrated in three different task scenarios highlighting the advantage of each stiffness mode. In each demonstration, the manipulator is actively bent with same control input (i.e. same number of incremental rotations of the tendon-driving motor) in a specific direction before and after a stiffness transition to highlight different behaviors.

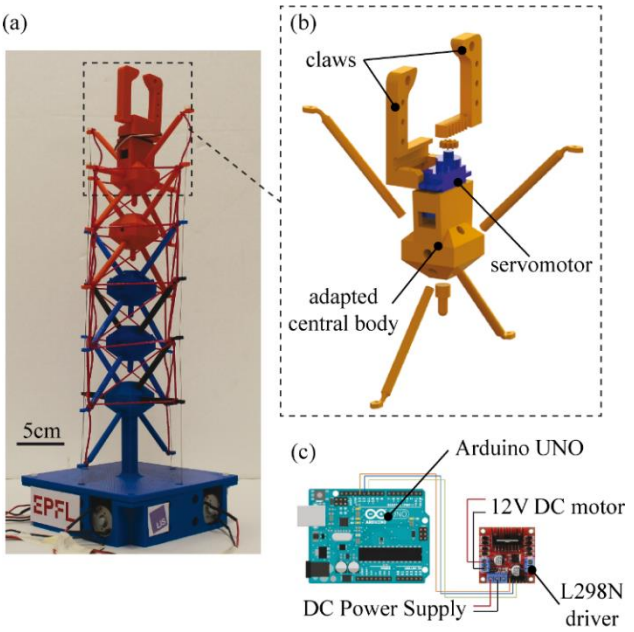

Figure 5. The continuous manipulator design with a 5 vertebrae variable-stiffness tensegrity spine (a). In blue, the 3 original vertebrae of the characterized spine segment in orange the 2 additional vertebrae. The top vertebra is modified with a built-in gripper composed of two claws actuated by a servo-motor (b). Schematics of the electronics to allow open loop user control (c).

1. *Soft mode*: the manipulator is capable of complying with objects while moving in its workspace to demonstrate safe interaction with the environment (Figure 6(a))
2. *Stiff mode*: the manipulator is capable of lifting a heavy object (i.e. 300 grams) thanks to increased stiffness to demonstrate on-demand load-bearing capability (Figure 6(b)).
3. *Directional stiff mode*: the manipulator is capable of lifting a heavy object (i.e. 300 grams) in the vertical plane (i.e. orthogonal to the table surface) and safely comply with objects in the horizontal plane (i.e parallel to the table surface) to demonstrate load-bearing capability and compliance in different directions (Figure 6(c)).

VI. CONCLUSIONS AND FUTURE WORK

We proposed a novel variable-stiffness tensegrity spine capable of transitioning among three different stiffness modes. The mechanical adaptability given by the three stiffness modes has been validated in a proof-of-concept continuous tensegrity manipulator capable of manipulating heavy objects and complying with obstacles while moving. Moreover, the stiffness is independently variable in two different orthogonal planes.

Here, the variable-stiffness is achieved by actively adding or removing a ball joint constrain among the vertebrae

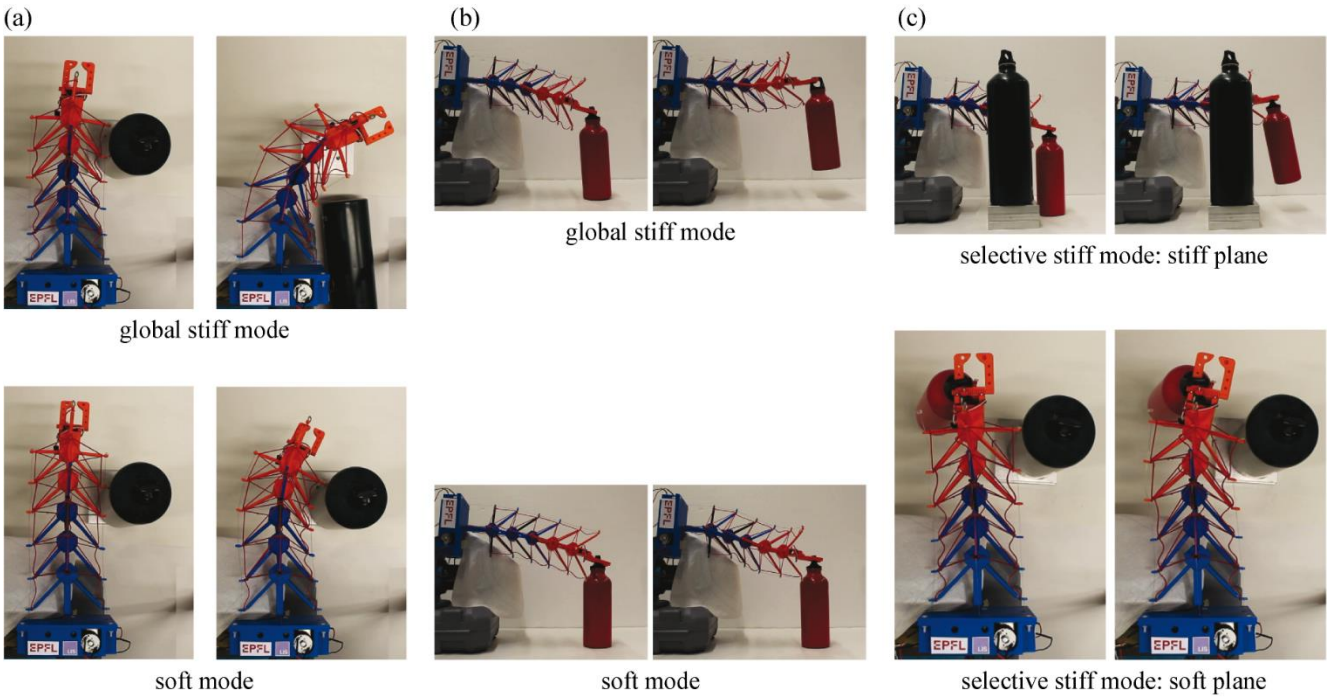

Figure 6. (a) Top view of the manipulator clamped at one side and placed horizontally to a table surface. A bottle weighting around 500 grams is placed in its reachable workspace. A sequence of two images show the manipulator bending on the right while in global stiff mode (top) and in soft mode (bottom). In the first case, the manipulator is too stiff and pushes the bottle to fall on the table, while in the soft mode the manipulator is able to comply with the bottle avoiding its fall on the table. (b) Side view of the manipulator clamped at one side and placed horizontally to a table surface while grasping a bottle weighting 300 grams. A sequence of two images show the manipulator bending upwards while in global stiff mode (top) and in soft mode (bottom). In the first case the manipulator is able to lift the bottle. In the second its stiffness is not sufficient to transmit a high enough force to lift the bottle. (c) Lateral view and top view of the manipulator clamped on one side and standing horizontally to a table surface. A bottle weighting around 300 grams is grasped by the gripper, while a bottle weighting around 500 grams is placed in its reachable workspace. The manipulator is in selective stiff mode, the plane orthogonal to the table surface is stiff while the parallel plane is soft. In the two top images of the sequence, the manipulator is able to lift the bottle in its stiff plane. In the two bottom images of the sequence, while the manipulator is lifting the bottle, it bends on the right in its soft plane and it is able to comply with the second bottle avoiding its fall on the table.

by means of tendon driven actuation system. The mechanism allows to change the tensegrity system class from a *class 1* with no constrain between the rigid bodies to a *class 2* with ball-joints constraints among the vertebrae. In the future, more advanced modelling or use of optimization algorithms [25-26] may allow to increase the morphological and mechanisms space design in terms of stiffness range and workspace. Furthermore, more reliable manufacturing techniques, such as molding instead of 3D printing, could improve the quality of the elastic cables to match the stiffness of the uniform cross-section cables of the model.

The current version of the variable-stiffness tensegrity spine has its actuators in a rigid base at the bottom of the first vertebrae. Even if this mechanical solution may be suitable for a continuous manipulator which always needs an attachment point at its base, in the future different designs could be developed embedding the actuators in the first vertebrae or by replacing passive cables with artificial muscles [27]. These alternative actuation mechanisms could better suit the integration of the variable-stiffness tensegrity spine in bio-inspired mobile robots such as quadrupeds, humanoids, crawling and swimming robots. Moreover, adding encoders and other sensing capabilities could allow a close control loop of the variable-stiffness tensegrity spine and its robotic applications. Finally, the manipulator described here has a modular design and multiple vertebrae can be added to increase length and workspace. Moreover, different types of end-effectors may be mounted on its top vertebrae.

We believe that the variable-stiffness tensegrity spine described here could represent a powerful core for the next generation of robots that display the mechanical flexibility and adaptability of biological vertebrates.

APPENDIX

A supporting video can be found in the supplementary material.

ACKNOWLEDGMENTS

This work was supported by the Swiss national Science Foundation through the FLAG ERA RoboCom++ project, and by the SNSF Bridge project 20B2-1_180861.

REFERENCES

1. Coyle S, Majidi C, LeDuc P, Hsia KJ. Bio-inspired soft robotics: Material selection, actuation, and design. Extreme Mechanics Letters. 2018 Jul 1;22:51–9.

2. Manti M, Cacucciolo V, Cianchetti M. Stiffening in Soft Robotics: A Review of the State of the Art. IEEE Robotics Automation Magazine. 2016 Sep;23(3):93–106.
3. Kowalski RJ, Ferrara LA, Benzel EC. Biomechanics of the Spine. In 2005.
4. Potvin JR, McGILL SM, Norman RW. Trunk Muscle and Lumbar Ligament Contributions to Dynamic Lifts with Varying Degrees of Trunk Flexion. Spine. 1991 Sep;16(9):1099.
5. Levin SM. The tensegrity-truss as a model for spine mechanics: biotensegrity. J Mech Med Biol. 2002 Sep 1;02(03n04):375–88.
6. Georgilas I, Tourassis V. From the Human Spine to Hyperredundant Robots: The ERMIS Mechanism. International Scholarly Research Notices. 2013:1-9.
7. Kim Y, Cheng S, Kim S, Iagnemma K. A Stiffness-Adjustable Hyperredundant Manipulator Using a Variable Neutral-Line Mechanism for Minimally Invasive Surgery. IEEE Transactions on Robotics. 2014 Apr;30(2):382–95.
8. Park Y-J, Cho K-J. Design and Manufacturing a Bio-inspired Variable Stiffness Mechanism in a Robotic Dolphin. In: Lee J, Lee MC, Liu H, Ryu J-H, editors. Intelligent Robotics and Applications. Springer Berlin Heidelberg; 2013. p. 302–9. (Lecture Notes in Computer Science).
9. Yeo SH, Yang G, Lim WB. Design and analysis of cable-driven manipulators with variable stiffness. Mechanism and Machine Theory. 2013 Nov 1;69(Supplement C):230–44.
10. Walker ID. Continuous Backbone " Continuum " Robot Manipulators: A Review. In 2013:1-20.
11. Sabelhaus AP, van Vuuren LJ, Joshi A, Zhu E, Garnier HJ, Sover KA, et al. Design, Simulation, and Testing of a Flexible Actuated Spine for Quadruped Robots. arXiv:180406527 [cs]. 2018 Apr 17.
12. Sabelhaus AP, Ji H, Hylton P, Madaan Y, Yang C, Agogino AM, et al. Mechanism Design and Simulation of the ULTRA Spine: A Tensegrity Robot. In: Volume 5A: 39th Mechanisms and Robotics Conference. Boston, Massachusetts, USA: American Society of Mechanical Engineers; 2015. p. V05AT08A059.
13. Mirletz BT, Park I-W, Flemons TE, Agogino AK, Quinn RD, SunSpiral V. Design and Control of Modular Spine-Like Tensegrity Structures. :10.
14. Mirletz BT, Bhandal P, Adams RD, Agogino AK, Quinn RD, SunSpiral V. Goal-Directed CPG-Based Control for Tensegrity Spines with Many Degrees of Freedom Traversing Irregular Terrain. Soft Robotics. 2015 Dec 1;2(4):165–76.
15. Furet M, Chablat D, Fasquelle B, Khanna P, Chevallereau C, Wenger P. Prototype of a tensegrity manipulator to mimic bird necks. 2019;10.
16. Oliveira MC, Skelton RE. Tensegrity Systems. Boston, MA: Springer US; 2009.
17. Zappetti D, Mintchev S, Shintake J, Floreano D. Bio-inspired Tensegrity Soft Modular Robots. In: Biomimetic and Biohybrid Systems. Springer, Cham; 2017. p. 497–508. (Lecture Notes in Computer Science).
18. Chen L-H, Daly MC, Sabelhaus AP, Janse van Vuuren LA, Garnier HJ, Verdugo MI, et al. Modular Elastic Lattice Platform for Rapid Prototyping of Tensegrity Robots. In American Society of Mechanical Engineers Digital Collection; 2017.
19. Mirletz BT, Park IW, Quinn RD, SunSpiral V. Towards bridging the reality gap between tensegrity simulation and robotic hardware. In: 2015 IEEE/RSJ International Conference on Intelligent Robots and Systems (IROS). 2015. p. 5357–63.
20. BulletPhysicsEngine, http://www.bulletphysics.org/, 2013.
21. Lessard S, Bruce J, Jung E, Teodorescu M, SunSpiral V, Agogino A. A lightweight, multi-axis compliant tensegrity joint. In: 2016 IEEE International Conference on Robotics and Automation (ICRA). 2016. p. 630–5.
22. Kim K, Agogino AK, Moon D, Taneja L, Toghyan A, Dehghani B, et al. Rapid prototyping design and control of tensegrity soft robot for locomotion. In: 2014 IEEE International Conference on Robotics and Biomimetics (ROBIO 2014). 2014. p. 7–14.
23. Caluwaerts K, Despraz J, Işçen A, Sabelhaus AP, Bruce J, Schrauwen B, et al. Design and control of compliant tensegrity robots through simulation and hardware validation. Journal of The Royal Society Interface. 2014 Sep 6;11(98):20140520.
24. Simple 3d printed 9g servo gripper, https://www.thingiverse.com/thing:2302957, 2017.
25. Morzadec T, Marcha D, Duriez C. Toward Shape Optimization of Soft Robots. In: 2019 2nd IEEE International Conference on Soft Robotics (RoboSoft). 2019. p. 521–6.
26. Howard D, Eiben AE, Kennedy DF, Mouret J-B, Valencia P, Winkler D. Evolving embodied intelligence from materials to machines. Nat Mach Intell. 2019 Jan;1(1):12–9.
27. Mirvakili SM, Hunter IW. Artificial Muscles: Mechanisms, Applications, and Challenges. Advanced Materials. 2018;30(6):1704407.